

DEVELOPING FREQUENCY-DOMAIN MODELS FOR NONLINEAR CIRCUITS BASED ON LARGE-SIGNAL MEASUREMENTS*

Jeffrey Jargon¹, K.C. Gupta², Dominique Schreurs³, and Donald DeGroot¹

¹*National Institute of Standards and Technology*

325 Broadway, M/S 813.01, Boulder, CO 80305, USA | E-mail: jargon@boulder.nist.gov

²*University of Colorado at Boulder, Boulder, CO 80309, USA*

³*Katholieke Universiteit Leuven, B-3001 Leuven, BELGIUM*

ABSTRACT

We describe an approach for generating artificial neural network (ANN) models for nonlinear devices, based upon frequency-domain data measured using a nonlinear vector network analyzer (NVNA). We demonstrate that these ANN models give accurate descriptions of the input-output relationships of the device over the span of the measurements. We also use the models to construct application-specific engineering figures of merit using appropriate ratios of wave variables measured under large-signal conditions. We obtain an independent check by comparing diode-circuit models, generated by means of this methodology, to a compact model simulated in commercial harmonic-balance software.

INTRODUCTION

Although the measurement of S -parameters using a vector network analyzer (VNA) is invaluable to the microwave designer of linear circuits, such measurements are oftentimes inadequate for nonlinear circuits since nonlinearities transfer energy from the stimulus frequency to products at new frequencies. Thus, a different and more sophisticated instrument is required to measure nonlinear devices and circuits. A recently introduced nonlinear vector network analyzer (NVNA) is capable of providing accurate waveform vectors by acquiring and correcting the magnitude and phase relationships between the fundamental and harmonic components in the periodic signals [1-5]. An NVNA excites a nonlinear device under test (DUT) with one or more sine-wave signals and detects the response of the DUT at its signal ports. Assuming the DUT exhibits neither sub-harmonic nor chaotic behavior, the input and output signals will be combinations of sine-wave signals, due to the nonlinearity of the DUT combined with mismatches between the system and the DUT.

Even though S -parameters cannot adequately represent nonlinear circuits, some type of parameters relating incident and reflected signals are beneficial so that the designer can “see” application-specific engineering figures of merit that are similar to what he or she is accustomed to. In this paper, we propose definitions of such ratios that we refer to as nonlinear large-signal \mathfrak{S} -parameters. We construct these parameters from artificial neural network (ANN) models that are trained with multiple frequency-domain measurements made on a nonlinear DUT with an NVNA.

In the following sections, we define nonlinear large-signal \mathfrak{S} -parameters, and describe the method for generating them using ANNs. We then compare a diode circuit model, generated using this method, to a harmonic balance simulation of a commercial device model. We conclude that these nonlinear large-signal \mathfrak{S} -parameters can be applied to the design of nonlinear devices and circuits.

A similar approach has been used in reference [6] where ‘nonlinear scattering functions’ were introduced by linearizing the nonlinear behavior around the operating point of a bipolar transistor used in a power amplifier. The formulation presented here does not involve any linearization and presents the designer with parameters that readily give physical insight.

NONLINEAR LARGE-SIGNAL SCATTERING PARAMETERS

Like commonly used linear S -parameters, nonlinear large-signal \mathfrak{S} -parameters can also be defined as ratios of reflected and incident wave variables. However, unlike linear S -parameters, nonlinear large-signal \mathfrak{S} -parameters depend upon the input signal magnitude and must take into account the total harmonic content of the signals since power will be transferred to other frequencies in a nonlinear device.

*Work of U.S. Government, not subject to U.S. Copyright.

In this paper we will consider a two-port device excited at port 1 by a single-tone signal (a_{11}) at a frequency f_1 . This condition is commonly encountered with power amplifiers and frequency doublers, although the approach can be generalized to any number of ports with multiple excitations that are harmonically related. In this case, we define an input reflection coefficient as

$$\mathfrak{S}_{11k1} = \frac{|b_{1k}| \angle \left(\phi_{b_{1k}} - k\phi_{a_{11}} \right)}{|a_{11}|} \left| a_{mn} = 0 \text{ for } \forall m \forall n [(m \neq 1) \wedge (n \neq 1)] \right. , \quad (1)$$

where a_{jl} (port j , spectral component number l) and b_{ik} (port i , spectral component number k) refer to the complex incident and scattered traveling voltage waves, respectively, and \mathfrak{S}_{ijkl} indicates the nonlinear large-signal \mathfrak{S} -parameter. Instead of simply taking the ratio of b_{1k} to a_{11} , we phase normalize to a_{11} . To do this we must subtract k times the phase of a_{11} ($\phi_{a_{11}}$) from that of b_{1k} ($\phi_{b_{1k}}$). The limitation imposed on the equation is that all other incident waves other than a_{11} equal zero. Another valuable parameter, the forward transmission coefficient, is similarly defined as

$$\mathfrak{S}_{21k1} = \frac{|b_{21k}| \angle \left(\phi_{b_{21k}} - k\phi_{a_{11}} \right)}{|a_{11}|} \left| a_{mn} = 0 \text{ for } \forall m \forall n [(m \neq 1) \wedge (n \neq 1)] \right. . \quad (2)$$

This parameter provides the designer with a value of the gain or loss through a device, either at the fundamental frequency, or converted to a higher harmonic frequency.

In addition to the previous two parameters, an output reflection coefficient can also be useful when trying to determine the output matching network. When a nonlinear DUT is operating under a normal drive condition (a_{11} at some constant signal level), we define a quasi-linear reflection coefficient at port 2 as

$$\mathfrak{S}_{22kk} = \frac{\Delta b_{2k}}{\Delta a_{2k}} \left| \text{Large } a_{11}, \text{ Small } \Delta a_{2k} \right. , \quad (3)$$

where a small pilot tone Δa_{2k} , generated by a second source at port 2, is offset slightly from the frequency of interest f_k by Δf_k . Equation (3) is very similar to the concept of ‘‘Hot S_{22} ,’’ which has been used to measure the degree of mismatch at the output port of a power amplifier at its excitation frequency [7].

METHODOLOGY

The nonlinear large-signal \mathfrak{S} -parameters defined above cannot be determined directly from measurements on a currently available NVNA, since impedance mismatches and harmonics from the source cannot be entirely eliminated in these instruments. The nonlinear DUT, in conjunction with the impedance mismatches and harmonics from the source make it impossible to set all of the a 's other than a_{11} (assuming port 1 excitation) to zero. In order to overcome this obstacle, we propose a method that makes use of multiple measurements of the DUT using a second source and couplers. This measurement set-up was that introduced by Verspecht et al. [6] to generate ‘nonlinear scattering functions.’

To illustrate our technique, let us consider the case when a DUT is excited at port 1 by a single-tone signal at frequency f_1 and signal level $|a_{11}|$. Utilizing a second source, multiple measurements of a nonlinear circuit are taken for different values of a_{mn} $[(m \neq 1) \wedge (n \neq 1)]$. These data are then used to develop an ANN model that maps values of a 's to b 's. The nonlinear large-signal \mathfrak{S} -parameters are obtained from the ANN model by interpolating b 's, obtained from measured results for nonzero values of a_{mn} $[(m \neq 1) \wedge (n \neq 1)]$, to the desired values for a_{mn} $[(m \neq 1) \wedge (n \neq 1)]$ equal to zero, or alternatively another condition called for by the desired application-specific figure of merit.

The ANN architecture used for this modeling is a feedforward, three-layer perceptron structure (MLP3) consisting of an input layer, a hidden layer, and an output layer [8]. The hidden layer allows complex models of input-output relationships. In this study, we utilized software developed by Zhang et al. [9] to construct the ANN models.

MEASUREMENTS, TRAINING, AND COMPARISON

To test our method of generating nonlinear large-signal \mathfrak{S} -parameters, we fabricated a wafer-level test circuit using a Schottky diode in a series configuration in the middle of gold coplanar waveguide (CPW) transmission lines etched on an alumina substrate. We measured the test circuit on an NVNA using an on-wafer line-reflect-reflect-match (LRRM) VNA calibration, along with signal amplitude and phase calibrations [5]. This process places the reference plane at the tips of the wafer probes used to connect with the CPW leads.

For all measurements, the first source, located at port 1, was set to a sine-wave excitation of frequency 900 MHz and magnitude $|a_{11}| \approx 0.178$ V (-5 dBm in a 50Ω environment) at the probe tips. The second source was connected to port 2 and was set to a sine-wave excitation of frequency 900 MHz and $|a_{21}| \approx 0.178$ V. The diode was forward-biased to $+0.2$ V through the probe tips. In order to obtain the nonlinear large-signal \mathfrak{S} -parameters, \mathfrak{S}_{11k1} and \mathfrak{S}_{21k1} , the excitation from source 1 was held constant, while the phase of source 2 was randomly changed for 250 different measurements that varied slightly in magnitude. Figure 1 plots the resulting measurements of a_{21} in the complex plane. The nonlinearities in the test circuit, along with impedance mismatches, created other input components at higher harmonics, which varied in magnitude and phase around the origin. These variations in a_{ij} allowed us to create an ANN model that could be used to interpolate b 's from the measured results for nonzero values of $a_{mn} [(m \neq 1) \wedge (n \neq 1)]$ to the desired values for $a_{mn} [(m \neq 1) \wedge (n \neq 1)]$ equal to zero, or alternatively another desired device condition.

Data from the 250 measurements were used to develop two ANN models, one for mapping values from the first five harmonics of a_1 and a_2 ($a_{11}, a_{12}, \dots, a_{15}, a_{21}, a_{22}, \dots, a_{25}$) to the first five harmonics of b_1 ($b_{11}, b_{12}, \dots, b_{15}$), and the other for mapping values from the first five harmonics of a_1 and a_2 to the first five harmonics of b_2 ($b_{21}, b_{22}, \dots, b_{25}$). An independent set of 250 points were used as testing data. The testing error for b_{11} through b_{15} was 0.72% and for b_{21} through b_{25} was 0.78%, with respective correlation coefficients of 0.99997 and 0.99989.

Once the ANN models were developed, the nonlinear large-signal \mathfrak{S} -parameters, \mathfrak{S}_{11k1} and \mathfrak{S}_{21k1} ($k = 1, 2, \dots, 5$), were obtained from eqs. (1) and (2) by interpolating b_{1k} and b_{2k} from measured results for nonzero values of $a_{12}, a_{13}, \dots, a_{15}$ and $a_{21}, a_{22}, \dots, a_{25}$ to the desired values for $a_{12}, a_{13}, \dots, a_{15}$ and $a_{21}, a_{22}, \dots, a_{25}$ equal to zero. Figure 2 shows the interpolated value of b_{11} ($= \mathfrak{S}_{1111} \cdot a_{11}$) when $a_{12}, a_{13}, \dots, a_{15}$ and $a_{21}, a_{22}, \dots, a_{25}$ were set equal to zero.

We compared our results to a compact model provided by the manufacturer and simulated in commercial harmonic-balance software to get an independent check on our methodology. Our comparison was accomplished by providing the simulator with the identical biasing conditions on the diode and a stimulus of the same magnitude used in the measurements for a_{11} and setting all other a 's to zero. Providing the simulated circuit with a_{11} of the same magnitude as the measurement should give the same values of b_{1k} and b_{2k} as the interpolated values of b_{1k} ($= \mathfrak{S}_{11k1} \cdot a_{11}$) and b_{2k} ($= \mathfrak{S}_{21k1} \cdot a_{11}$) determined by the ANN models when $a_{12}, a_{13}, \dots, a_{15}$ and $a_{21}, a_{22}, \dots, a_{25}$ are set equal to zero. Figure 2 shows that the simulated value b_{11} agrees with that determined from the measurement-based ANN model. Quantitatively, the differences between the ANN and equivalent-circuit models are shown in Table 1.

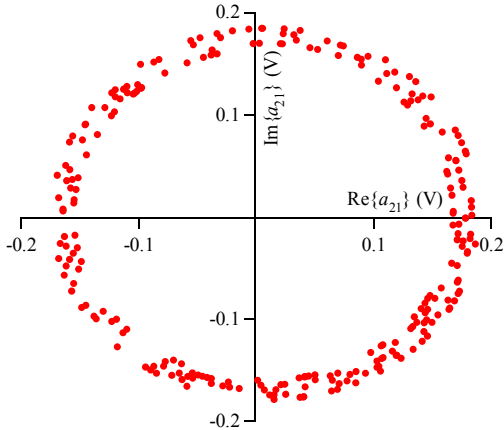


Figure 1. Measurements of a_{21} in the complex plane with the excitation from source 1 held constant and the output from source 2 set to random phases with constant amplitude.

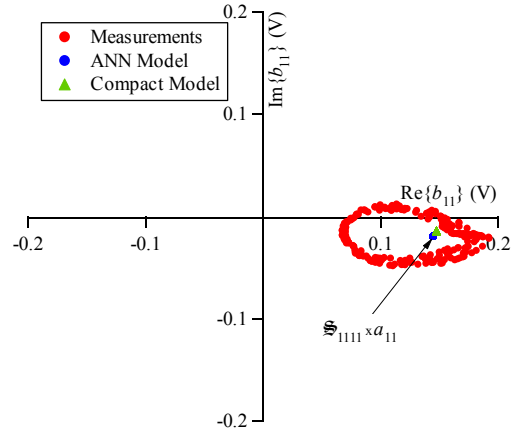


Figure 2. Measurements of b_{11} in the complex plane. Values of $\mathfrak{S}_{1111} \cdot a_{11}$ were determined from the measurement-based ANN model and the harmonic balance simulation using a compact model.

Table 1. Differences between the measurement-based, ANN-modeled results and the compact model simulated in commercial harmonic-balance software.

Quantity	Difference (%)	Difference (dBV)	Quantity	Difference (%)	Difference (dBV)
\mathcal{S}_{1111}	3.38	-44.5	\mathcal{S}_{2111}	3.95	-43.2
\mathcal{S}_{1121}	1.23	-53.3	\mathcal{S}_{2121}	7.15	-38.0
\mathcal{S}_{1131}	3.29	-44.8	\mathcal{S}_{2131}	5.93	-39.6
\mathcal{S}_{1141}	0.40	-63.1	\mathcal{S}_{2141}	0.72	-57.9
\mathcal{S}_{1151}	1.67	-50.6	\mathcal{S}_{2151}	0.85	-56.5

CONCLUDING REMARKS

We described a method of generating nonlinear large-signal scattering parameters (\mathcal{S}_{ijkl}), using an NVNA equipped with a second source. Multiple measurements of a nonlinear circuit were used to train artificial neural networks that yield portable models, independent of the measurement instrumentation. We checked our approach by comparing our results to a compact model simulated in commercial harmonic-balance software, and showed that the two methods agree well.

Advantages of developing such frequency-domain models for nonlinear circuits include the ability to link model accuracy to measurements, the ability to “see” engineering figures of merit, and the possible elimination of the transformation from time-domain to frequency-domain currently required in harmonic-balance analysis to accelerate simulation time.

There are many possible applications of nonlinear large-signal \mathcal{S} -parameters. For example, the source impedance required for conjugate match (maximum power transfer) at the excitation frequency of a nonlinear device may be obtained from \mathcal{S}_{1111} by specifying the large-signal operating point. Similarly, \mathcal{S}_{2211} can be used to select the optimum output load impedance at the fundamental frequency in a power amplifier. Values of \mathcal{S}_{2211} could also be obtained, not only for a specified input power level (a_{11}), but also for specified terminations at various harmonics (a_{2k}/b_{2k}). In addition to power-amplifier applications, \mathcal{S}_{22kk} could also be used to select the optimum load impedance for the output at the k th harmonic for a frequency multiplier. We are currently investigating applications and generalizations of nonlinear large-signal \mathcal{S} -parameters, including representing them as impedance and admittance parameters, and will report on our progress.

ACKNOWLEDGEMENTS

The authors thank Q. J. Zhang of Carleton University for his support with the neural network software, Kate Remley of NIST for providing us with the data simulated using harmonic-balance, and Jan Verspecht and Marc Vanden Bossche of Agilent Technologies for their helpful discussions and instrumentation support. Dominique Schreurs is supported by the Fund for Scientific Research-Flanders as a post-doctoral fellow.

REFERENCES

- [1] M. Sipila, K. Lehtinen, V. Porra, “High-frequency periodic time-domain waveform measurement system,” *IEEE Trans. Microwave Theory Tech.*, vol. 36, pp. 1397-1405, Oct. 1988.
- [2] U. Lott, “Measurement of magnitude and phase of harmonics generated in nonlinear microwave two-ports,” *IEEE Trans. Microwave Theory Tech.*, vol. 37, pp. 1506-1511, Oct. 1989.
- [3] G. Kompa and F. Van Raay, “Error-corrected large-signal waveform measurement system combining network analyzer and sampling oscilloscope capabilities,” *IEEE Trans. Microwave Theory Tech.*, vol. 38, pp. 358-365, Apr. 1990.
- [4] J. Verspecht, P. Debie, A. Barel, and L. Martens, “Accurate on wafer measurement of phase and amplitude of the spectral components of incident and scattered voltage waves at the signal ports of a nonlinear microwave device,” *1995 IEEE MTT-S Int. Microwave Symp. Dig.*, vol. 3, pp. 1029-1032, May 1995.
- [5] J. Verspecht, “Calibration of a measurement system for high-frequency nonlinear devices,” Doctoral Dissertation, Vrije Universiteit Brussel, Belgium, 1995.
- [6] J. Verspecht and P. Van Esch, “Accurately characterizing hard nonlinear behavior of microwave components with the nonlinear network measurement system: introducing nonlinear scattering functions,” *Proc. 5th Annual Workshop on INMMC*, pp.17-26, Duisburg, Germany, Oct. 1998.
- [7] J. Browne, “System automates power-amp testing,” *Microwaves & RF*, pp. 213-220, Dec. 1999.
- [8] Q. J. Zhang and K. C. Gupta, *Neural Networks for RF and Microwave Design*, Artech House, 2000.
- [9] NeuroModeler, ver. 1.2, Q. J. Zhang and his neural network research team, Department of Electronics, Carleton University, Ottawa, Canada, 1999.